



Correlation Analysis Between Urban Heat Island Intensity and Temperature Criticality Value in Denpasar City

I Ketut Gede Arta Putra, Idung Risdiyanto, Rahmat Hidayat

Department of Geophysics and Meteorology, Faculty of Mathematics and Natural Sciences, IPB University, Dramaga Campus, Bogor, Indonesia 16680

ARTICLE INFO

Received

17 January 2023

Revised

24 March 2023

Accepted for Publication

11 April 2023

Published

25 July 2023

doi: [10.29244/j.agromet.37.2.66-76](https://doi.org/10.29244/j.agromet.37.2.66-76)

Correspondence:

I Ketut Gede Arta Putra
Department of Geophysics and Meteorology, Faculty of Mathematics and Natural Sciences, IPB University, Dramaga Campus, Bogor, Indonesia 16680
Email: arta_putrasss@apps.ipb.ac.id

This is an open-access article distributed under the CC BY License.

© 2023 The Authors. *Agromet*.

ABSTRACT

The compactness of buildings in Denpasar results in the formation of urban heat islands (UHI), which can be evaluated through the Urban Thermal Field Variance Index (UTFVI) and Environment Criticality Index (ECI). ECI was the ratio of land surface temperature to the Normalized Difference Vegetation Index (NDVI). It can be transformed into Temperature Criticality Value (TCV) using air temperature and Index-based Built-up Index (IBI). This study aims to identify the UHI intensity, the impact of land cover changes, and its association with the TCV in Denpasar, Bali. The study employed Landsat 8 imagery combined with field measurements data. The results demonstrated that land cover in Denpasar was mainly built-up areas that had grown from 2015 to 2021. The UTFVI value confirmed the increased built-up areas as indicated by the intense UHI (>0.02), whereas the mean value of NDVI suggested a reduction in vegetation density. The density of built-up areas (IBI) had increased, while vegetation had decreased. The TCV value for 2015 until 2021 suggested the increased critical environment condition. A transect analysis revealed that stronger UHI intensity, denser buildings, and a more critical environment were present in urban centers compared to the suburbs. The correlation coefficient (r) between TCV and UTFVI was relatively robust (0.75–0.82), indicating that the growth of UHI intensity was associated with a more critical environment. TCV had a strong correlation ($r > 0.80$) with Built-up Index but inverse correlation with NDVI. Therefore, limiting the expansion of built-up areas and increasing vegetation could help to control the environment's criticality.

KEYWORDS

built-up area, environment conditions, Landsat 8, urban heating, vegetation density

INTRODUCTION

The transformation of vegetation into buildings can undoubtedly impact climate and environmental conditions, leading to an increase in urban air temperature due to changes in energy balance (Effendy et al., 2006; Li et al., 2022). This can result in the emergence of urban heat islands, which, when combined with alterations in land cover, can create hazardous conditions. These effects can be observed in all urban areas, including Denpasar City, the capital of Bali Province, which serves as a center for government and various employment opportunities (Hermanto et

al., 2018). Between 2014 and 2017, Denpasar City experienced a growth of 222.42 hectares in settlements and 241.4 hectares in industry, trade, and service zones. Unfortunately, this expansion has resulted in the loss of 178.54 hectares of mangroves, urban forests, and 263.63 hectares of agriculture (Pratiwi and Citra, 2019).

Research conducted by Zal et al., (2017) revealed a 7.65% reduction in vegetation between 2003 and 2015 in Denpasar City, contributing to a 1.7°C increase in air temperature. Using building materials that reflect radiation more efficiently can also lead to a rise in the temperature of the surrounding air. On the other hand, vegetation can utilize solar energy during photo-

synthesis, releasing less heat and cooler air temperatures (Yuan et al., 2021). Therefore, the conversion of vegetation to built-up areas can have a significant impact on the rise in air temperature.

Urban development had the potential to create the urban heat island (UHI) phenomenon, which was characterized by an increase in air temperatures, as noted by Zahro et al., (2018). The UHI phenomenon refers to the temperature difference between the urban core and the surrounding suburbs, forming an island-like spatial pattern (Lauriola, 2016). In areas affected by UHI, the air temperature is higher in the city center and decreases as it moves toward rural areas, according to Simwanda et al., (2019). Estimating the intensity of UHI is crucial because it can demonstrate how variations in air temperature impact critical environmental variables.

Ranagalage et al., (2017) used the Environmental Criticality Index (ECI) to spatially evaluate the critical environment caused by increasing surface temperatures and decreasing vegetation. As Sharma et al., (2017) note, the assessment of environmental criticality had evolved to consider additional parameters such as built-up area and land wetness, in addition to surface temperature and vegetation index. Currently, the ECI still converts the value of each parameter into a digital number (DN), which represents the numeric value (byte) of each pixel in the image and typically ranges from 0-255 (Jaya et al., 2021). This study transformed the ECI into a Temperature Criticality Value (TCV) based on the air temperature parameter and an Index-based Built-up Index (IBI) to measure the built-up area.

This study aims to investigate the potential formation of urban heat islands (UHI) in Denpasar City and its ecological implications by developing an environmental criticality assessment methodology using the Temperature Criticality Value (TCV). This research seeks to accomplish three primary objectives: firstly, to determine the severity of the UHI phenomenon; secondly, to assess the impact of land cover changes on UHI intensity; and thirdly, to examine the correlation between UHI and the temperature criticality value (TCV) in Denpasar City.

RESEARCH METHODS

Data Source

The data used in this research were Landsat 8 OLI/TIRS satellite imagery, the daily air temperature data from the Ngurah Rai Meteorological Station in January 2022, and field measurement data. The satellite imagery from Landsat 8 OLI/TIRS was collected in April 2015, April 2018, and June 2021, with a spatial resolution of 30 m for visible bands and 100 m for thermal bands. The field data were collected using a standard Hygrometer to measure the air temperature

(°C) and an infrared thermometer to measure surface temperature (°C) from January to March 2022.

Image Processing

The data processing steps involved in this study consisted of various techniques such as the Maximum Likelihood method for supervised land cover classification, transforming the vegetation density index, extracting surface temperature, and estimating air temperature. The vegetation density was analyzed using the Normalized Difference Vegetation Index (NDVI) derived from the near-infrared (NIR) and red bands of the satellite imagery, as per Sharma et al., (2017). The land surface temperature was extracted using the split-window (SW) algorithm using bands 10 and 11 of the Landsat 8 image, following Equation 1 developed by Rongali et al., (2018). The air temperature was estimated by converting the land surface temperature using the sensible heat from the energy balance component, as per Equation 2 (Wiweka, 2014).

$$LST = TB_{10} + C_1(TB_{10} - TB_{11}) + C_2(TB_{10} - TB_{11})^2 + C_0 + (C_3 + C_4W)(1 - m) + (C_5 + C_6W)\Delta m \quad (1)$$

$$T_a = LST - \frac{r_a \times H}{\rho_a \times C_p} \quad (2)$$

where LST was land surface temperature (°C), TB was brightness temperature (°C), C_0 - C_6 was split-window coefficients, m was mean emissivity, Δm was emissivity difference, W was total atmospheric water vapor content (0.013 g/cm^2), T_a was air temperature (°C), r_a was aerodynamics density, H was latent heat flux (Wm^{-2}), ρ_a was air density (1.27 kg m^{-3}), and C_p was heat capacity ($1004 \text{ J kg}^{-1} \text{ K}^{-1}$).

Field Measurements

To obtain data measurements, transects were distributed from the city center to rural areas. The number of samples (n) for each transect line pixel (N) was determined using the Slovin method with an error tolerance of 0.1 (Equation 3). The Slovin method was suitable for determining the number of samples based on a purposive pattern, in this case, following the transects pattern. However, the number of the population used must be known. The field data was collected through measurements of surface temperature, air temperature, and land cover conditions. These measurements were used to verify the accuracy of the image data processing results.

$$n = \frac{N}{1 + Ne^2} \quad (3)$$

Data Accuracy Test

The land cover classification accuracy was evaluated using overall accuracy and kappa statistics (Equation 4 and Equation 5) (Sampurno and Thoriq, 2016). To eliminate the effect of measurement time,

surface temperature and air temperature were normalized using a sinusoidal function (Monteith and Unsworth, 2013). The air temperature was normalized to 2.23 UTM according to the image data. The accuracy of surface temperature was assessed using the determination coefficient, while the accuracy of air temperature estimation was evaluated by comparing the data distribution of each land cover, the transect pattern, and measuring the Normalized Mean Absolute Error (NMAE) (Zahro et al., 2018).

$$\text{Overall accuracy(\%)} = \frac{\sum_i^r X_{ii}}{N} \times 100\% \quad (4)$$

$$\text{Kappa(\%)} = \frac{N \sum_i^r X_{ii} - \sum_i^r X_{i+} X_{+i}}{N^2 - \sum_i^r X_{i+} X_{+i}} \times 100\% \quad (5)$$

where X_{ii} was the number of reference pixels that corresponds to land use classification pixel, X_{+i} was the number of pixels resulting from land use classification, X_{+i} was the number of pixels of land use reference, r was number of land use classes, and N was the number of all reference pixels.

Parameters Analysis

The parameter analysis in this research involved identifying the urban heat island (UHI) phenomenon, the Index-based Built-up Index (IBI), the Temperature Criticality Value (TCV), and analyzing the relationship between each parameter. UHI was analyzed by classifying air temperature and the Urban Thermal Field Variance Index (UTFVI) (Equation 6). Air temperature values were classified based on their mean and standard deviation (Amindin et al., 2021). Where T_a represented air temperature ($^{\circ}\text{C}$), and T_m represented mean air temperature ($^{\circ}\text{C}$). The analysis of the relationship between each parameter involved evaluating the impact of changes in land cover on the intensity of UHI and investigating the correlation between UHI and the TCV in Denpasar City.

$$\text{UTFVI} = \frac{T_a - T_m}{T_m} \quad (6)$$

The IBI (Equation 7) was created by combining the Normalized Difference Built-up Index (NDBI), which serves as the base of the built-up index (Equation 8), the Normalized Difference Vegetation Index (NDVI) as the vegetation index (Equation 9), and the Modified Normalized Difference Water Index (MNDWI) as the wetness index (Equation 10). This built-up index is more sensitive to pixels representing water bodies and vegetated land. NDBI was derived from a combination of short-wave infrared (SWIR) and near-infrared (NIR) bands, while MNDWI was obtained from the green and SWIR bands (Xu et al., 2013).

$$\text{IBI} = \frac{\text{NDBI} - \frac{\text{NDVI} + \text{MNDWI}}{2}}{\text{NDBI} + \frac{\text{NDVI} + \text{MNDWI}}{2}} \quad (7)$$

$$\text{NDBI} = \frac{\text{SWIR1} - \text{NIR}}{\text{SWIR1} + \text{NIR}} \quad (8)$$

$$\text{NDVI} = \frac{\text{NIR} - \text{Red}}{\text{NIR} + \text{Red}} \quad (9)$$

$$\text{MNDWI} = \frac{\text{Green} - \text{SWIR1}}{\text{Green} + \text{SWIR1}} \quad (10)$$

The Temperature Criticality Value (TCV) was a modification of the Environmental Criticality Index (ECI) used to identify critical environmental conditions. In a study by Sasmito and Suprayogi, (2018), ECI was measured using land surface temperature and Built-up Index (BU), which was the difference between NDBI and NDVI (Equation 11). Another study by Sharma et al., (2017) added the wetness index (NDWI) to ECI, but this approach stretched the parameters and ignored the temperature factor (Equation 12). TCV was developed to improve the ECI results by replacing BU with IBI, including the wetness factor and adjusting the surface temperature to air temperature, directly impacting human activities (Equation 13). TCV was defined as the critical air temperature value in degrees Celsius that results from the impact of built-up land compaction on the built-up index ($^{\circ}\text{C} \cdot \text{IBI}$).

$$\text{ECI} = \text{LST} \times \text{BU} = \text{LST} \times (\text{NDBI} - \text{NDVI}) \quad (11)$$

$$\text{ECI} = \frac{\text{LST} + \text{NDBI}}{\text{NDVI} + \text{NDWI}} \quad (12)$$

$$\text{TCV} = T_a \times \text{IBI} \quad (13)$$

where LST was surface temperature ($^{\circ}\text{C}$) and T_a was air temperature ($^{\circ}\text{C}$).

To identify the critical area, TCV was divided into 5 classes with threshold values based on the average value and standard deviation, as was the case with the UHI classification in Table 1 (Amindin et al., 2021).

Table 1. Temperature Criticality Value (TCV) classification and its threshold value.

Class of TCV	Threshold
Very Good	$\text{TCV} \leq \text{TCV}_m - 1.5\text{std}$
Good	$\text{TCV}_m - 1.5\text{std} < \text{TCV} \leq \text{TCV}_m - \text{std}$
Moderate	$\text{TCV}_m - \text{std} < \text{TCV} \leq \text{TCV}_m + \text{std}$
Critical	$\text{TCV}_m + \text{std} < \text{TCV} \leq \text{TCV}_m + 1.5\text{std}$
Very critical	$\text{TCV} > \text{TCV}_m + 1.5\text{std}$

The distribution of UTFVI, IBI, and TCV was analyzed by examining their patterns along the transects from the city center to rural areas. This analysis aimed to determine how these parameters were distributed in different areas. Additionally, the relationship between these parameters was evaluated using a correlation test. Correlation test used to assess the strength of association between two or more variables (Azhari et al., 2017).

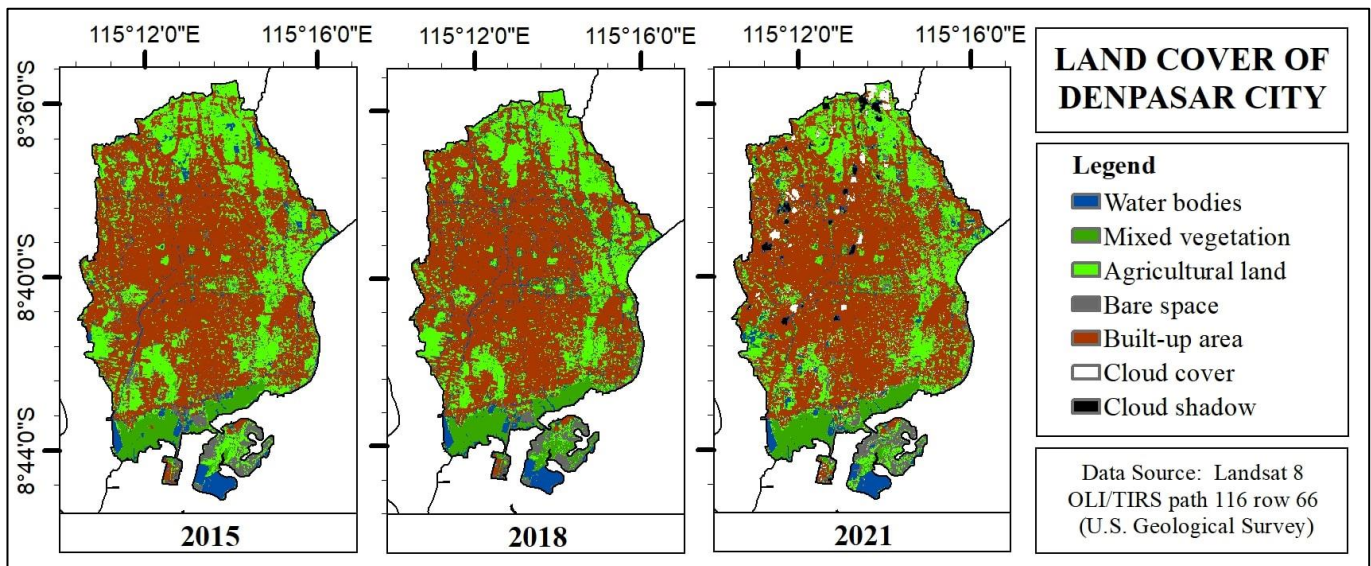


Figure 1. The land cover distribution on Denpasar City for 2015, 2018, and 2021 based on Landsat imagery.

RESULTS AND DISCUSSION

Land Cover Changes

During the three years of observation, Denpasar City was dominated by built-up areas, as showed in Figure 1. Water bodies such as bays, reservoirs, and rivers were presented, and mixed vegetation (dominated by mangroves) and agricultural land were mostly distributed in the suburbs. There was minimal bare space area. In the 2021 classification, clouds and their shadows were removed during the quantification process.

The land cover analysis showed that the area of water bodies and mixed vegetation increased from 2015 to 2018, but decreased in 2021. Conversely, the bare space area fell in 2018 but raised in 2021. The built-up area had the highest increase, from 54.70% in 2015 to 59.35% in 2021, while agricultural land had the highest degradation, decreasing from 27.00% in 2015 to 22.16% in 2021. The transformation of land cover types was observed, with water bodies being transformed into agricultural land (20.17%) and built-up areas (13.81%); mixed vegetation into built-up areas (18.06%); agricultural land into bare space (11.32%) and built-up areas (12.14%); and plain space into agricultural land (20.29%) and built-up areas (17.18%).

The conversion of built-up areas to agricultural and bare space was minimal, accounting for less than 2% of the total. On the other hand, there was a significant conversion of land cover to built-up areas, totaling 792.52 hectares, while agricultural land was degraded by 1137.10 hectares. The land cover classification showed an overall accuracy rate of 94.01%, indicating excellent results. The kappa value obtained was 87.34%, classified as almost perfect agreement.

Therefore, the classification results can be considered representative of the study area (Alkaradaghi et al., 2018).

Land Surface Temperature

The surface temperature of Denpasar City exhibited a range from 28°C to 40.5°C in 2015, 22.9°C to 40.4°C in 2018, and 24.9°C to 40.8°C in 2021. The maximum surface temperature increased, but the minimum surface temperature decreased from 2015 to 2021. Urban centers had warmer surface temperatures than the suburbs. The coefficient of determination (R^2) between the estimated surface temperature and field measurements was found to be 0.953 for water bodies, 0.802 for mixed vegetation, 0.621 for agriculture, 0.845 for bare space, and 0.605 for built-up areas. This indicates a one-way relationship between the estimated surface temperature from the image and the field measurements. The image estimation matched the pattern of the field measurements, indicating it was reliability for further analysis.

Air Temperature

Urban centers in Denpasar City had warmer air temperatures than suburban areas, predominantly covered by vegetation. Although the maximum temperature remained relatively stable throughout the three observation years, the minimum temperature in 2018 was lower than in the other years. To compare the air temperature distribution between field measurements and image estimations, the 2021 image estimation results were analyzed, assuming minimal land cover changes (Figure 2). The image estimation showed a more distributed air temperature pattern than the field observations, with similar pattern.

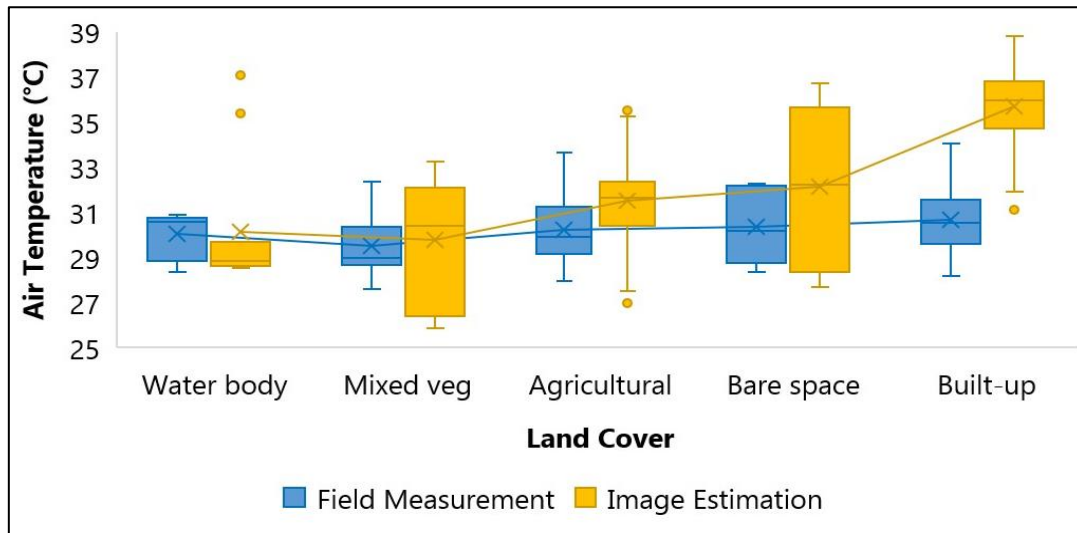


Figure 2. Variation of air temperature (°C) for each land cover from field measurement and image estimation. Box-plot indicates Q1, median, Q3, and dots represent outliers with whisker in percents 10% and 90% quantile.

The field measurements and image estimation data results indicated that the average air temperature was highest in the built-up area, followed by bare space. The densest air temperature distribution in both field measurements and image estimation was found in water bodies. The air temperature pattern observed in each transect was similar, with temperatures increasing in urban centers and decreasing in the suburbs. The Normalized Mean Absolute Error (NMAE) values for water bodies, mixed vegetation, agriculture, bare space, and built-up areas were 7.18%, 7.69%, 8.27%, 6.61%, and 16.84%, respectively. The overall error rate was 14.32%, less than 30%, indicating that the data were representative of the study area and can be used for further analysis (Zahro et al., 2018).

Urban Heat Island

According to the air temperature classification, there was an increased in the very cold air temperature

category in Denpasar City in 2021, as shown in Figure 3. The UHI phenomenon, indicated by a pattern of hot and very hot air temperatures resembling an island in the city center, had been presented since 2015. However, the air temperature in the very hot category had decreased each year of observation. In contrast areas with moderate air temperature conditions had expanded as very cold and cold air temperatures had decreased.

Accorded to Figure 4, the UHI intensity in the study area increased from 2015 to 2018 but decreased in 2021. This increase could be attributed to the growth of built-up areas with a lower albedo and higher heat storage capacity than vegetated land. It can also be observed that UHI intensity was higher in urban centers compared to suburban areas and tended to occur more in built-up areas than in vegetated land. The UTFVI can be divided into six classes, ranging from non-UHI to

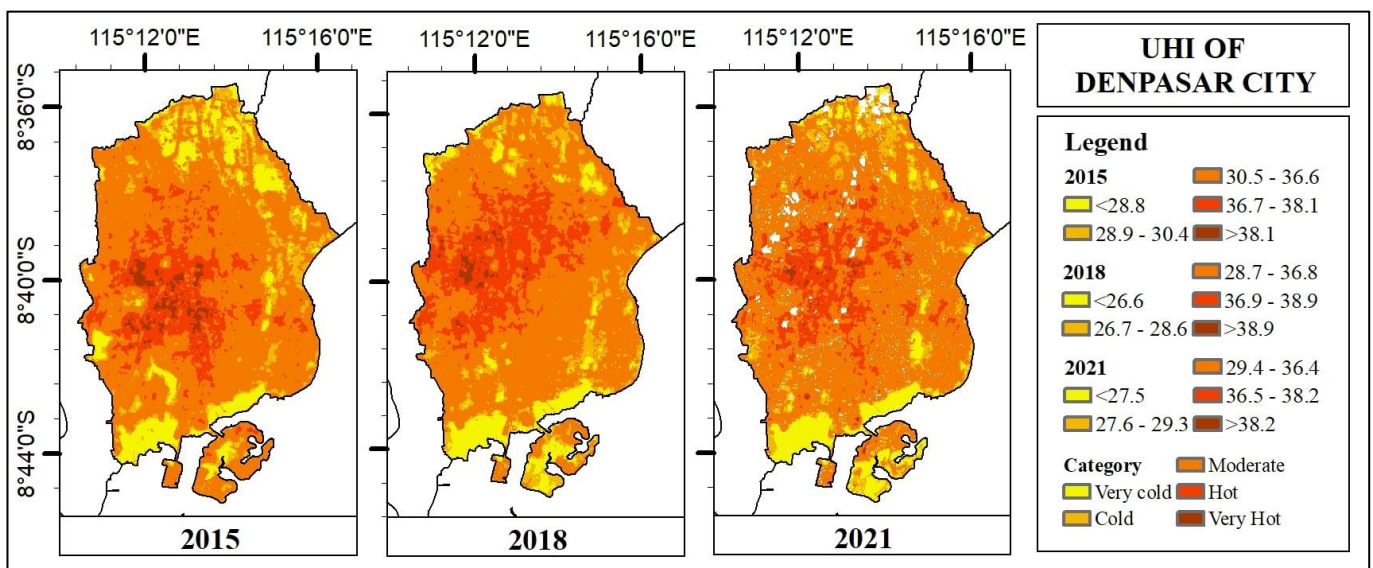


Figure 3. Urban Heat Island (UHI) distribution of Denpasar City in 2015, 2018, and 2021.

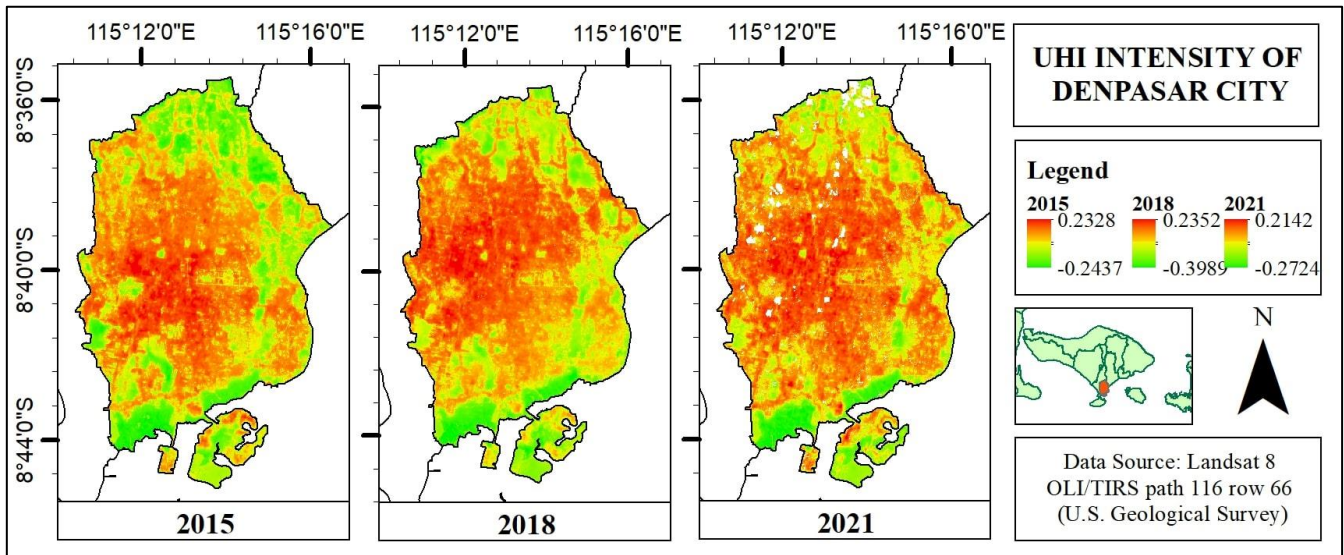


Figure 4. Urban Heat Island (UHI) intensity distribution based on Urban Thermal Field Variance Index (UTFVI) of Denpasar City in 2015, 2018, and 2021.

strongest UHI. The study area had a dominant presence of the strongest UHI (>50%) and non-UHI space (>40%) in the three years of observation. Areas with the strongest intensity expanded during this period, unlike non-UHI areas. Although the UHI intensity decreased in 2021, it was essential to address this issue as the study area still had a dominant presence of the strongest UHI, which can have adverse effects on the environment and human health.

Vegetation Index (NDVI)

The vegetation index in Denpasar City showed a decrease in vegetation density from 2015 to 2021, as evidenced by the range of values for each year and the reduction in mean NDVI distribution. The data distribution was positively skewed due to the higher frequency of rare vegetation data compared to dense vegetation data. The NDVI was classified into water

bodies, bare soil, sparse vegetation or built-up areas, moderate vegetation, and dense vegetation. Denpasar was dominated by sparse vegetation or built-up areas, which increased yearly. The percent of moderate and dense vegetation, representing green open spaces, was very low, less than 1% in 2018 and 2021. The total area of green open spaces decreased to 20.03% in 2021.

Built-up Index (IBI)

The IBI (Index-based Built-up Index) values in Denpasar City for 2015 ranged from -0.431 to 0.178, for 2018 went from -0.392 to 0.187, and for 2021 went from -0.418 to 0.189. The maximum IBI value indicated increasing compacted built-up areas in Denpasar City. The average IBI distribution also showed an increase in building density every year of observation. The distribution of IBI data was opposite to that of NDVI, which had a negative skewness due to the median

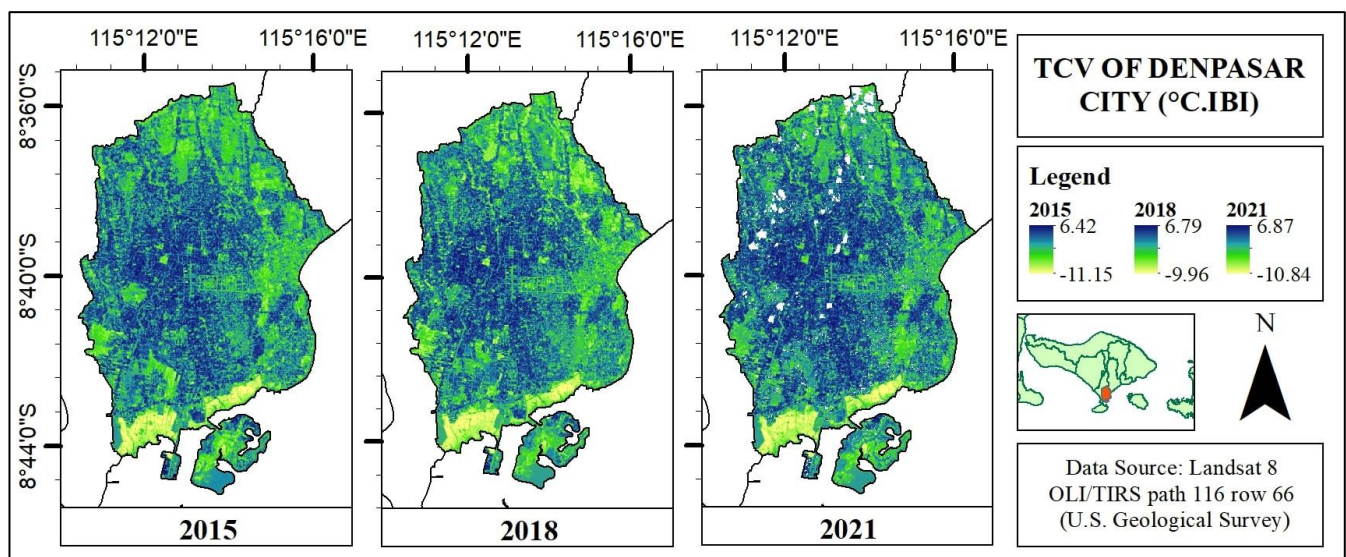


Figure 5. Temperature Criticality Value (TCV) of Denpasar City in 2015, 2018, and 2021.

Table 2. The Temperature Criticality Value (TCV) threshold and its corresponding area in Denpasar City for 2015, 2018, and 2021.

Class of TCV	2015		2018		2021	
	Threshold	Area (ha)	Threshold	Area (ha)	Threshold	Area (ha)
Very Good	< -5.26	1,026.71	< -5.59	1,138.01	< -5.16	1,142.39
Good	-5.26 - -3.89	1,308.78	-5.59 - -4.32	1,177.65	-5.16 - -3.82	1,035.98
Moderate	-3.89 - 1.56	7,025.46	-4.32 - 0.78	8,052.91	-3.82 - 1.56	8,162.26
Critical	1.56 - 2.93	2,889.09	0.78 - 2.05	1,815.52	1.56 - 2.91	1,865.01
Very critical	> 2.93	329.96	> 2.05	395.91	> 2.91	374.37

value being more significant than the average. This indicated that there was more data above the average (denser built-up areas) than below the average (less dense built-up areas). The bottom outliers in the IBI distribution were water bodies and dense mixed vegetation.

Temperature Criticality Value (TCV)

The TCV in Denpasar City had increased every year of observation, indicating a more critical environment (Figure 5). The built-up areas had a higher TCV and were more essential than the vegetated areas. The average distribution of TCV also increased, suggesting a worsening of the environment. The data distribution had a negative skewness, indicating that there were more areas with TCV above the average (more critical) than below the average. The lower outlier was dense vegetation, while the top outlier in 2018 was built-up areas.

The threshold for TCV was determined based on the classification of air temperature in the UHI analysis, as described by Amindin et al., (2021). The study area was dominated by moderate TCV, which had expanded every year of observation. The area with very good TCV also grew, but the conditions of good and critical TCV tended to decrease. The area with critical TCV fluctuated during the three years of observation, increasing in 2018 and decreasing in 2021. The pattern of changes in TCV was almost identical to that of UHI distribution. When areas with very hot air temperatures decrease, areas with critical TCV also decrease (Table 2).

The Relationship Between TCV with UBU, IBI, and Forming Index

The transect analysis of Denpasar City for each

parameter highlighted the differences between the city center and suburban areas (Figure 7). The south-north transect demonstrated that the city center area had higher parameter values than suburban areas, primarily due to the dominance of built-up areas, mangroves in the south, and agricultural land in the north. On the west transect, the parameter values were higher than on the east transect, mainly due to the high density of built-up areas. The suburban area on the southwest transect had a low value due to the presence of water bodies, while the northeast area comprises agricultural land. On the northwest-southeast transect, the TCV and IBI parameters did not exhibit significant differences, but the UTFVI increased in the city center, while the suburban areas in the southeast had low values due to mangrove cover. The pattern indicated that the center to the west area, which was predominantly built-up, had a stronger UHI intensity and a more critical environment compared to suburban areas dominated by vegetation, in line with previous research (Khan et al., 2021; Ranagalage et al., 2017; Sharma et al., 2017).

The correlation between TCV and built-up indices such as NDBI and IBI was strong and positive ($r=0.99$), indicating that an increase in the built-up area led to a more critical environment. Conversely, NDVI and TCV showed a robust negative relationship, suggesting that reducing vegetation density leads to a necessary environment. While UTFVI and TCV had a strong relationship, it was not as strong as that between TCV and the built-up factor. The wetness factor (MNDWI) does not have a significant inverse relationship with TCV and only represents the condition of water bodies. The p -value < 0.05 for the correlation of each parameter for three different years indicated that the relationship

Table 3. Correlation coefficient and p -value each parameter for three years observation.

Year	TCV-UTFVI		TCV-IBI		TCV-NDVI		TCV-MNDWI		TCV-NDBI	
	r	p -value	r	p -value	r	p -value	r	p -value	r	p -value
2015	0.80	0.001	0.99	0.000	-0.85	0.000	-0.43	0.000	0.99	0.000
2018	0.75	0.000	0.99	0.000	-0.84	0.001	-0.45	0.000	0.99	0.000
2021	0.82	0.000	0.99	0.000	-0.81	0.000	-0.49	0.000	0.99	0.000

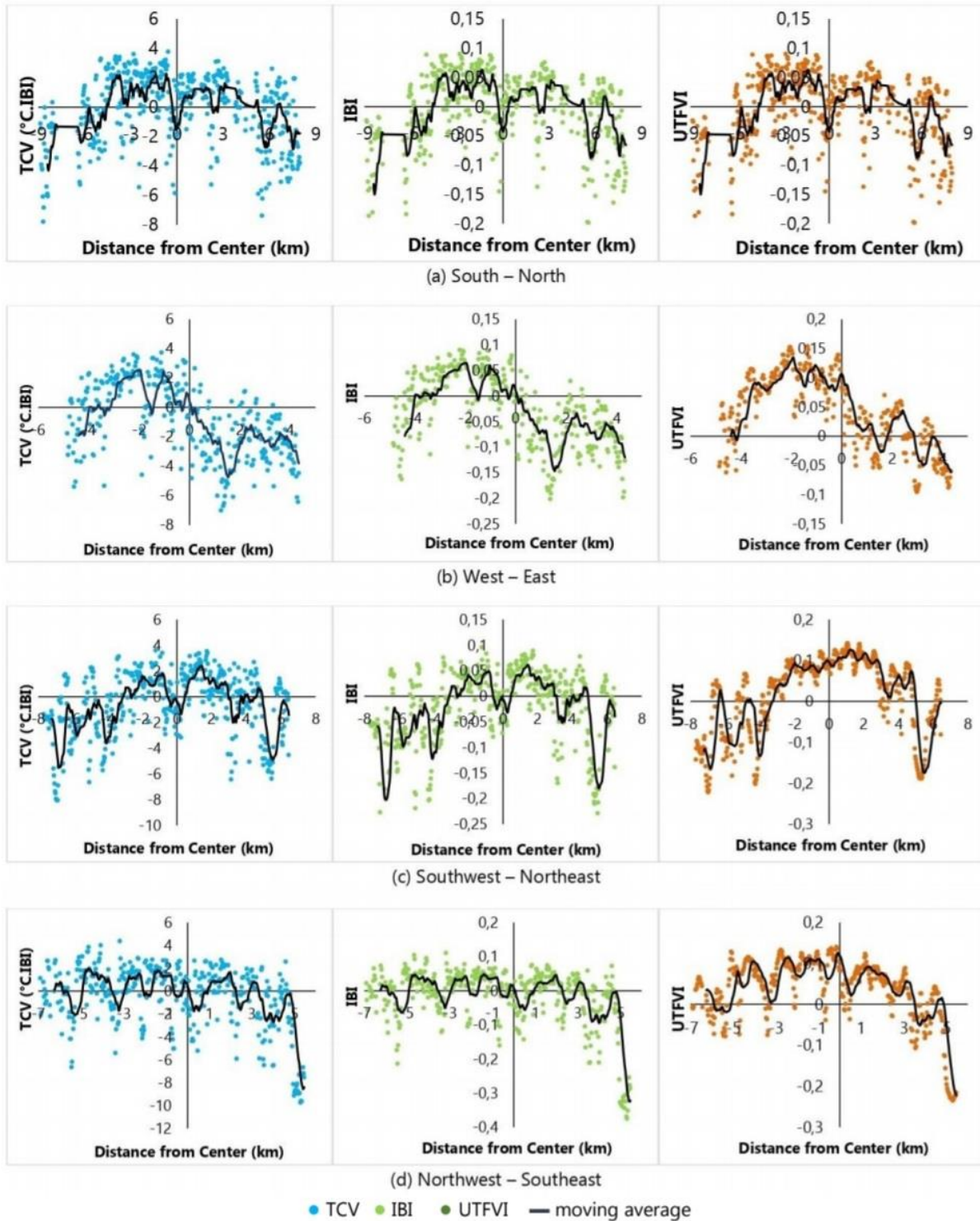


Figure 6. Transects pattern of Temperature Criticality Value (TCV), Built-up Index (IBI), Urban Thermal Field Variance Index (UTFVI), and moving average.

between TCV and other parameters was significant, with a low statistical test error (Azhari et al., 2017).

Discussion

The conversion of agricultural land to bare space and built-up areas was a significant cause of land degradation in Denpasar City. According to BAPPEDA Kota Denpasar (2019), the city experienced a 35 ha

decrease in irrigated agricultural fields between 2013 and 2017 due to land conversion. This trend had continued, with built-up areas now dominating at 62.22% and agricultural land accounting for only 29.22% of the land cover in 2021 (Arcana et al., 2021). However, accurately identifying land cover changes through image classification was challenging, as there can be similarities in pixel tones, particularly between

water bodies, agricultural land, and mixed vegetation. The resulting land cover changes significantly impact urban thermal conditions, particularly surface and air temperatures.

Urban areas with more built-up areas tended to had warmer surface and air temperatures than suburban areas dominated by vegetation which tend to be more relaxed. Urban thermal dynamics were influenced by various meteorological factors closely linked to changes in land cover, and one of these factors was albedo. Albedo referred to the ratio of reflected short-wave radiation to that absorbed at the earth's surface (Falasca et al., 2019), and surfaces with higher albedo values reflect more radiation, which in turn leads to an increase in air temperature due to the addition of sensible and latent heat in the atmosphere (Ghosh et al., 2018). Surfaces covered with building materials such as concrete, asphalt, and cement had a higher albedo value than vegetation, meaning that they reflect more radiation (Shamsudeen et al., 2022). Vegetation had cooling properties that regulate urban temperatures through evapotranspiration, which removes latent heat at near-surface temperatures. Additionally, the shading of the vegetation canopy also reduces radiation input to the surface, contributing to the cooling effect (Richards et al., 2020).

According to field measurements and image estimation, the highest average air temperature was found in built-up areas, while the lowest was found in areas with vegetation. This relationship between air temperature and land cover was consistent, with built-up areas having higher temperatures and vegetation having lower temperatures, as reported by Mukmin et al., (2016). Although image estimation produced higher values than field measurements, the normalized mean absolute error (NMAE) was less than 30%, which was influenced by meteorological factors such as cloudiness, rainfall, and radiation, as noted by Avdan and Jovanovska, (2016). The presence of dense and thick clouds and the possibility of rain can decreased air temperature by reducing the amount of incoming solar radiation that heats the surface. Despite a small error in air temperature estimation through image analysis, it can still be used for analyzing the urban heat island (UHI) phenomenon, as meteorological factors such as cloud cover, precipitation, and radiation can influence the accuracy of the estimation.

Since 2015, Denpasar City had been experiencing the urban heat island (UHI) phenomenon, as evidenced by the presence of hot and very hot air temperature categories in the city center, which forms a pattern similar to an island. The most significant expansion of UHI was observed in areas with a decreased area without UHI, which could had been triggered by the

development of the built-up area, showed an inverse relationship (Naim and Kafy, 2021). The increase in UHI intensity was also linked with a decrease in the vegetation index and an increase in built-up index. The intensity of UHI was further amplified due to the reduction in the green space area and the building density (Tepanosyan et al., 2021).

Between 2015 and 2021, there was a decrease in the maximum and average value of NDVI. The decrease was associated with a reduction in green open space, indicated by the dense vegetation and medium areas classification, and an expansion of built-up areas, indicated by the sparse vegetation classification. This expansion of the built-up area was evident in the increased maximum value and average IBI. A study by Xi et al., (2019) also reported a similar inverse relationship between IBI and NDVI, where an increase in IBI was associated with a decrease in NDVI.

Land cover changes had been identified as the cause of UHI phenomena, which impact the critical environment (Yang et al., 2017). In this study, the necessary environment referred to the change in urban thermal conditions resulting from vegetation, buildings, and land wetness dynamics, as represented by the Temperature Criticality Value (TCV). The TCV scores were higher in city centers than in the suburbs. Additionally, the Environmental Criticality Index (ECI) tended to be higher in city centers with denser buildings. The pattern of the critical environment area was similar to the distribution of UHI based on air temperature classification, which tended to be higher in urban centers. The strong relationship between the critical environment and the UHI phenomenon was due to the dynamics of urban air temperature, which were influenced by land cover changes (Fadlin et al., 2020).

The transect pattern of UTFVI, IBI, and TCV parameters indicated that they were higher in the city center than in the suburbs, and TCV was strongly correlated with the built-up index (IBI and NDBI). This correlation was related to the albedo of the built-up land, which could increase the air temperature and strengthen the UHI intensity, resulting in a more critical environment. Similarly, the transect pattern and building compaction strongly correlated with a more critical environment (Khan et al., 2021). Although the correlation between NDVI and TCV was not as strong as the built-up index, it was still inversely proportional. The reduction of wetlands and vegetation could increase the environmental's criticality, disrupting the ecosystem's balance (Sharma et al., 2017). Therefore, there was a need to limit built-up land and harmoniously increase green open space to control UHI and environmental criticality.

CONCLUSIONS

The maximum UHI intensity increased in Denpasar City and was dominated by the strongest UHI areas that expanded. Stronger UHI dominates the city center composed of built-up areas than the suburban composed of vegetation. Moreover, the expansion of the built-up and the decrease of vegetation caused an increase in air temperature. The strongest UHI areas were associated with a more critical environment, as evidenced by the strong correlation between UTFVI and TCV. Building compaction was the most significant factor contributing to the critical environment, as indicated by the closer correlation between TCV and built-up indices such as IBI and NDBI. While the vegetation index (NDVI) strongly correlates with TCV, it was not as strong as the built-up index. It was inversely proportional, indicating that decreased vegetation was a caused of increasing criticality in the environment. Therefore, balancing limitations on built-up areas and adding green open space was necessary to control UHI and environmental criticality in Denpasar City.

ACKNOWLEDGEMENT

The authors thank to the anonymous reviewer for their valuable comments and suggestions during the review process. Also thank to the Division of Meteorology and Atmospheric Pollution FMIPA IPB University for its support to the first author to attend the international seminar ISS 2022.

REFERENCES

- Alkaradaghi, K., Ali, S.S., Al-Ansari, N., Laue, J., 2018. Evaluation of land use & land cover change using multi-temporal landsat imagery: A case study Sulaimaniyah Governorate, Iraq. *J. Geogr. Inf. Syst.* 10, 247–260. <https://doi.org/10.4236/jgis.2018.10.3013>.
- Amindin, A., Pouyan, S., Pourghasemi, H.R., Yousefi, S., Tiefenbacher, J.P., 2021. Spatial and temporal analysis of urban heat island using Landsat satellite images. *Environ. Sci. Pollut. Res.* 28, 41439–41450. <https://doi.org/10.1007/s11356-021-13693-0>.
- Arcana, I.K.F., Paturusi, S.A., Suarna, I.W., 2021. Analysis of the supporting capacity and supply capability of residential land in Denpasar City. *Ecotrophic* 15, 247–257.
- Avdan, U., Jovanovska, G., 2016. Algorithm for automated mapping of land surface temperature using LANDSAT 8 satellite data. *J. Sensors*, 1–8. <https://doi.org/10.1155/2016/1480307>.
- Azhari, A., Darundiati, Y., Dewanti, N., 2017. Studi korelasi antara faktor iklim dan kejadian demam berdarah dengue tahun 2011-2016. *Higea J. Public Heal. Res. Dev.* 1, 163–175.
- BAPPEDA Kota Denpasar, 2019. Rencana Kerja Pemerintah Daerah Semesta Berencana Kota Denpasar Tahun 2020. Badan Perencanaan Pembangunan Daerah Kota Denpasar, Denpasar(ID).
- Effendy, S., Bey, A., Zain, A.F.M., Santosa, I., 2006. Peranan ruang terbuka hijau dalam mengendalikan suhu udara dan urban heat island wilayah Jabotabek. *Agromet* 20, 23-33. <https://doi.org/10.29244/j.agromet.20.1.23-33>.
- Fadlin, F., Kurniadin, N., Prasetya, F.V.A.S., 2020. Analisis indeks kekritisian lingkungan di Kota Makassar menggunakan Citra Satelit LANDSAT 8 OLI / TIRS. *J Geodesi dan Geomatika* 03, 55–63.
- Falasca, S., Ciancio, V., Salata, F., Golasi, I., Rosso, F., Curci, G., 2019. High albedo materials to counteract heat waves in cities: An assessment of meteorology, buildings energy needs and pedestrian thermal comfort. *Build. Environ.* 163, 1–38. <https://doi.org/10.1016/j.buildenv.2019.10-6242>.
- Hermanto, S.S.A., Makalew, A.D.N., Sulistyantara, B., 2018. Hubungan antara perubahan tutupan lahan terhadap total penduduk yang dipengaruhi oleh fenomena urbanisasi di Bogor, Jawa Barat. *J. Lanskap Indones.* 10, 7–11. <https://doi.org/10.29244/jli.v10i1.17397>.
- Jaya, L.M.G., Suprayogi, A., Sudarsono, Hasbi, M., 2021. Identification of non-volcanic geothermal manifestation in North Konawe Regency Indonesia using land surface temperature of Landsat satellite image. *IOP Conf. Ser. Earth Environ. Sci.* 622. <https://doi.org/10.1088/1755-1315/622/1/012040>.
- Khan, M.S., Ullah, S., Chen, L., 2021. Comparison on land-use/land-cover indices in explaining land surface temperature variations in the city of beijing, china. *Land* 10, 1–20. <https://doi.org/10.3390/land10101018>.
- Lauriola, P., 2016. Introduction, in: Musco, F. (Ed.), *Counteracting Urban Heat Island Effects in a Global Climate Change Scenario*. The Springer, Venezia (IT), pp. xlvii–liii. <https://doi.org/10.1007/978-3-319-10425-6>.
- Li, H., Zhou, Y., Jia, G., Zhao, K., Dong, J., 2021. Quantifying the response of surface urban heat island to urbanization using the annual temperature cycle model. *Geosci. Front.* 13, 101–141. <https://doi.org/10.1016/j.gsf.2021.101141>.
- Monteith, J.L., Unsworth, M.H., 2013. *Principles of Environmental Physics*, 4th Editio. ed, Chemical Geology. Elsevier Ltd, Oxford (UK).

- Mukmin, S.A. Al, Wijaya, A.P., Sukmono, A., 2016. Analisis pengaruh perubahan tutupan lahan terhadap distribusi suhu permukaan dan keterkaitannya dengan fenomena urban heat island. *J. Geod. Undip* 5, 224–233.
- Naim, M.N.H., Kafy, A. Al, 2021. Assessment of urban thermal field variance index and defining the relationship between land cover and surface temperature in Chattogram city: A remote sensing and statistical approach. *Environ. Challenges* 4, 1–14. <https://doi.org/10.1016/j.envc.2021.100107>.
- Pratiwi, G.P.D.S., Citra, I.P.A., 2019. Dinamika dan kesesuaian arahan fungsi kawasan di Kota Denpasar. *J. Pendidik. Geogr. Undiksha* 7, 18–24. <https://doi.org/10.23887/jjpg.v7i1.20674>.
- Ranagalage, M., Estoque, R.C., Murayama, Y., 2017. An urban heat island study of the Colombo Metropolitan Area, Sri Lanka, based on Landsat data (1997-2017). *ISPRS Int. J. Geo-Information* 6, 1–17. <https://doi.org/10.3390/ijgi6070189>.
- Richards, D.R., Fung, T.K., Belcher, R.N., Edwards, P.J., 2020. Differential air temperature cooling performance of urban vegetation types in the tropics. *Urban For. Urban Green* 50, 1–7. <https://doi.org/10.1016/j.ufug.2020.126651>.
- Rongali, G., Keshari, A.K., Gosain, A.K., Khosa, R., 2018. Split-window algorithm for retrieval of land surface temperature using Landsat 8 thermal infrared data. *J. Geovisualization Spat. Analysis*, 2. <https://doi.org/10.1007/s41651-018-0021-y>.
- Sampurno, R., Thoriq, A., 2016. Klasifikasi tutupan lahan menggunakan citra Landsat 8 Operational Land Imager (OLI) di Kabupaten Sumedang. *J. Teknotan* 10, 61–70. <https://doi.org/10.24198/jt.vol10n2.9>.
- Sasmito, B., Suprayogi, A., 2018. Spatial Analysis of Environmental Critically due to Increased Temperature in the Built Up Area with Remote Sensing. *IOP Conf. Ser. Earth Environ. Sci.* 165, 1–11. <https://doi.org/10.1088/1755-1315/165/1/01-2011>.
- Senanayake, I.P., Welivitiya, W.D.D.P., Nadeeka, P.M., 2013. Remote sensing based analysis of urban heat islands with vegetation cover in Colombo city, Sri Lanka using Landsat-7 ETM+ data. *Urban Clim.* 5, 19–35. <https://doi.org/10.1016/j.uclim.2013.07.004>.
- Shamsudeen, M., Padmanaban, R., Cabral, P., 2022. Spatio-temporal analysis of the impact of landscape changes on vegetation and land surface temperature over Tamil Nadu. *Earth* 3, 614–638. <https://doi.org/10.3390/earth3020036>.
- Sharma, R., Joshi, P.K., Mukherjee, S., 2017. Analyzing trends of urbanization and concomitantly increasing environmental cruciality—a case of the cultural city, Kolkata, in: Hazra, S., Mukhopadhyay, A., Ghosh, A.R., Mitra, D., Ddhwal, V. (Eds.), *Environment and Earth Observation*. Springer International Publishing Switzerland, Cham (CH), pp. 215–227. https://doi.org/10.1007/978-3-319-46010-9_14.
- Simwanda, M., Ranagalage, M., Estoque, R.C., Murayama, Y., 2019. Spatial analysis of surface urban heat islands in four rapidly growing African cities. *Remote Sens.* 11, 1–20. <https://doi.org/10.3390/rs11141645>.
- Sobrino, J.A., Irakulis, I., 2020. A methodology for comparing the surface urban heat island in selected urban agglomerations around the world from Sentinel-3 SLSTR data. *Remote Sens.* 12, 1–29. <https://doi.org/10.3390/RS12122052>.
- Tepanosyan, G., Muradyan, V., Hovsepyan, A., Pinigin, G., Medvedev, A., Asmaryan, S., 2021. Studying spatial-temporal changes and relationship of land cover and surface Urban Heat Island derived through remote sensing in Yerevan, Armenia. *Build. Environ.* 187, 1–45. <https://doi.org/10.1016/j.buildenv.2020.107390>.
- Yang, C., He, X., Yan, F., Yu, L., Bu, K., Yang, J., Chang, L., Zhang, S., 2017. Mapping the Influence of Land Use/Land Cover Changes on the Urban Heat Island Effect—A Case Study of Changchun, China. *Sustainability* 9. <https://doi.org/10.3390/su9020312>.
- Wiweka, 2014. Pola suhu permukaan dan udara menggunakan citra Satelit Landsat Multitemporal. *J. Ecolab* 8, 11–22. <https://doi.org/10.20886-jklh.2014.8.1.11-22>.